

Mercerization of Cellulose. IV. Mechanism of Mercerization and Crystallite Sizes*

HISAO NISHIMURA[†] and ANATOLE SARKO,[‡] *Department of Chemistry and the Cellulose Research Institute, State University of New York, College of Environmental Science and Forestry, Syracuse, New York 13210*

Synopsis

Using the Guinier plot, the 200 reflection profile of ramie cellulose I was resolved into two components. One component represented a crystallite size of $\sim 20 \text{ \AA}$, and the other component represented a crystallite size of $\sim 61 \text{ \AA}$. These components were followed during the conversion of cellulose I to Na-cellulose I, in order to estimate the contribution of the smaller crystallites to the early rapid stage of conversion. From the intensity ratio of the two components, it appears that during the first $\sim 20\%$ conversion the formation of Na-cellulose I occurs mainly in the oriented amorphous regions of the fiber. Following this, up to $\sim 65\%$ conversion the destruction and transformation of small crystallites takes place. The small average size of the $\sim 20 \text{ \AA}$ crystallites, as well as their relatively high reactivity to alkali, appear to facilitate the conversion of the parallel-chain cellulose I structure to an antiparallel one.

INTRODUCTION

In the previous part of this series, results were presented which strongly suggested that alkali mercerization of cellulose begins in the amorphous regions of the fiber.¹ In controlled mercerization experiments, a rapid formation of Na-cellulose I was observed up to a conversion ratio of approximately 65%. During this process, the Na-cellulose I structure—the first alkali-cellulose complex in the mercerization sequence—crystallized without apparent reduction of the average crystallite size of the parent cellulose I structure. In the subsequent, slow stage of conversion, all of cellulose I was transformed to Na-cellulose I through a gradual disappearance of the cellulose I crystallites and a simultaneous increase in the size of the Na-cellulose I crystallites.

At the same time, the possibility that conversion may also begin in small crystallites could not be ruled out, because the destruction of small crystallites has little effect on the measured, average crystallite size. Generally, crystalline fibrous polymers exhibit a range of crystallite sizes, measured in directions normal to the chain axes. A lateral size distribution for ramie cellulose has been proposed.² The smaller crystallites are also much less perfect in comparison with the larger ones. This, coupled with the larger surface-to-volume ratio

*Part III of this series, Ref. 1.

[†]Permanent address: Research Center, Daicel Chemical Industries, Ltd., Himeji, 671-12 Japan.

[‡]To whom correspondence should be addressed.

of the smaller crystallites, renders the latter more susceptible to chemical attack such as occurs in alkali mercerization.

In an attempt to determine the possible significance of this mode of conversion, an X-ray diffraction line profile analysis of cellulose I was undertaken during its transformation to Na-cellulose I.

EXPERIMENTAL

X-Ray Diffraction. Refined ramie fibers were used as the source of cellulose I. The procedures for sample purification, specimen preparation, and X-ray diffraction have been described.¹ The specimens for mercerization and diffraction were mounted in glass capillary tubes in such a fashion that the use of a 3.5*N* NaOH solution resulted in a complete conversion of cellulose I to Na-cellulose I in 12 days. The X-ray diffraction diagrams were recorded periodically (on the average, every 12 h), and analyzed as described below. Typical diffraction diagrams of cellulose I, Na-cellulose I, and a sample in the process of conversion are shown in Figure 1 of the preceding paper in this series.¹

Line Profile Analysis. The equatorial intensity profiles of the diffraction diagrams were obtained using a Joyce-Loebl Recording Microdensitometer. The overlapping reflections of both cellulose I and Na-cellulose I were resolved into individual Gaussian components using a least-squares procedure.³ The method of resolution depended on the characteristics of the intensity profile and the content of the cellulose I and Na-cellulose I components in the sample. For Na-cellulose I, as well as its mixtures with cellulose I where it was the major component (group A), the main reflection of Na-cellulose I (at $2\theta = 20.5^\circ$) was resolved into three peaks (cf. Fig. 1). In other cases where Na-cellulose I was present only as a minor component (group B), this reflection was treated as a single Gaussian peak.

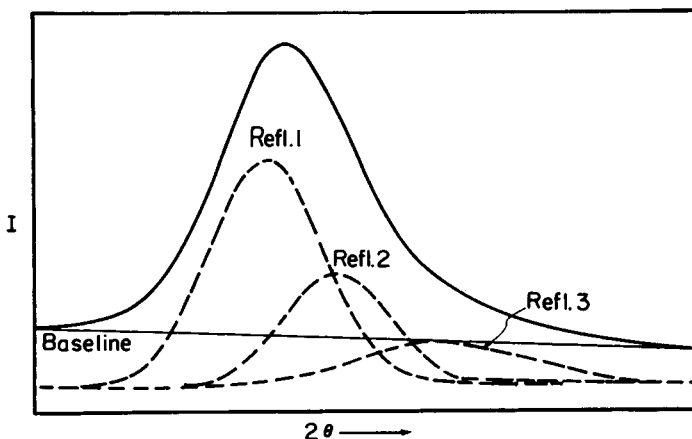


Fig. 1. Main equatorial reflection of Na-cellulose I and its resolution into three components. The observed intensity profile and its baseline are shown above the resolved peaks. The sum curve of the latter and the observed profile coincide exactly.

In all cases, the conversion ratio R , measuring the degree of conversion of cellulose I to Na-cellulose I, was calculated from the following equation:

$$R = 1 - \frac{\int I(2\theta)_{\text{cell I}} d(2\theta)}{\int I(2\theta)_{\text{total}} d(2\theta)} \quad (1)$$

where $I(2\theta)_{\text{cell I}}$ is the intensity due to all reflections of cellulose I, and $I(2\theta)_{\text{total}}$ is the combined intensity of cellulose I and Na-cellulose I (on the equator). The crystallite sizes were evaluated using the Scherrer peak-broadening formula:

$$L(hkl) = K/dS_p \quad (2)$$

where $L(hkl)$ is the crystallite size normal to the hkl plane, $K = 0.9$ for peak half-width measurements, and dS_p is the half-width of the Gaussian component curve. (The term "half-width" refers to the width of the reflection profile at half-height.) The values for dS_p were obtained and corrected as previously described.¹

RESULTS AND DISCUSSION

The equatorial intensity profile of an untreated ramie specimen is shown in Figure 2. The intense cellulose I (200) reflection was fitted with a single Gaussian line profile, and the best fit is shown in Figure 3. It is clear that a good fit cannot be obtained using a single Gaussian component, and that the deviation suggests the presence of a measure of Lorentzian character. (For this reason, the resolutions of diffraction line profiles of different celluloses into their individual components have generally required a linear combination of Gaussian and Lorentzian peak shapes.) The broadening of the base of the (200) reflection is not due to some other reflection, as the closest reflection to it on the high 2θ side is (020), whose intensity is negligible.⁴ Consequently, the deviation of the (200) reflection profile from a true Gaussian shape is likely to be a manifestation of a distribution of crystallite sizes. To test for this possibility, the (200) reflection profile was plotted in the form of a Guinier plot, with the intensity as $\log I(s)$ vs. s^2 (where $s = 2 \sin \theta / \lambda$). In this plot, the slope is determined by the electronic radius of gyration which can be taken as a measure of crystallite size.⁵ The resulting plot is shown in Figure 4, and it is clear that the curve exhibits two straight-line components, indicated by the two limiting slopes $I_{(200)S}$ and $I_{(200)L}$. From the slopes of these two lines, average crystallite dimensions of ~ 20 and ~ 61 Å, respectively, were calculated. The ~ 20 Å crystallites are quite small, of the order of only three times as large as the unit cell, but the existence of cellulose microfibrils in the 15–20 Å width range has been reported.⁶ The (200) reflection profile can thus be considered to be the resultant of two peaks—(200)S from the ~ 20 Å size crystallites, and (200)L from the ~ 61 Å crystallites. Using these dimensions, the resolutions of the (200) reflection of cellulose I, for both group A and group B diffraction patterns, are illustrated in Figures 5 and 6. The initial intensity ratio of $I_{(200)S}/I_{(200)L}$ was 0.184. The fit of the experimental profile and the sum of the two Gaussian peaks were good in all cases.

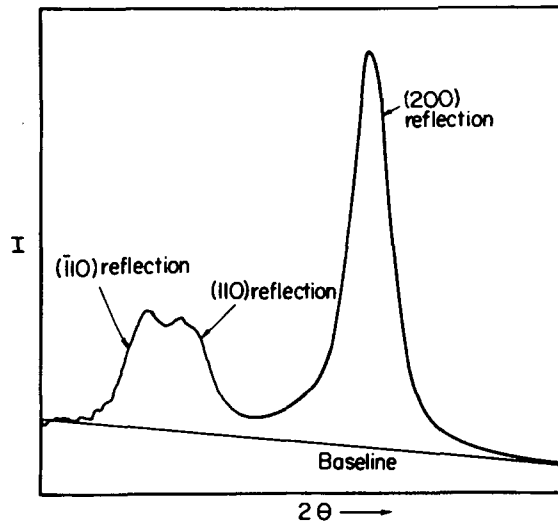


Fig. 2. Equatorial intensity profile of ramie cellulose I.

The results of this analysis, applied to the sample during the fast phase of conversion, are shown in Figure 7. The results are plotted as the ratio of intensities $I_{(200)S}/I_{(200)L}$ vs. the conversion ratio from 0 to 65%. It is clear that the intensity ratio decreases substantially with the increasing conversion ratio, indicating a decrease in the intensity component contributed by the small crystallites. It is also apparent that the decrease is nonlinear, proceeding slowly during the initial, 15–20% conversion phase, and increasing sharply at higher conversion ratios. This suggests that the conversion may indeed begin in the amorphous regions of the fiber—as was proposed earlier¹—but that, very soon thereafter, the conversion of small crystallites of cellulose I accounts for the majority of the transformation. Only after the small crystallites have

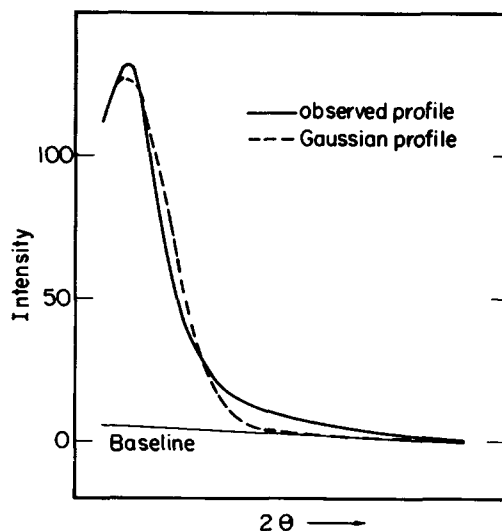


Fig. 3. Best fit of the (200) reflection profile of cellulose I with one Gaussian component.

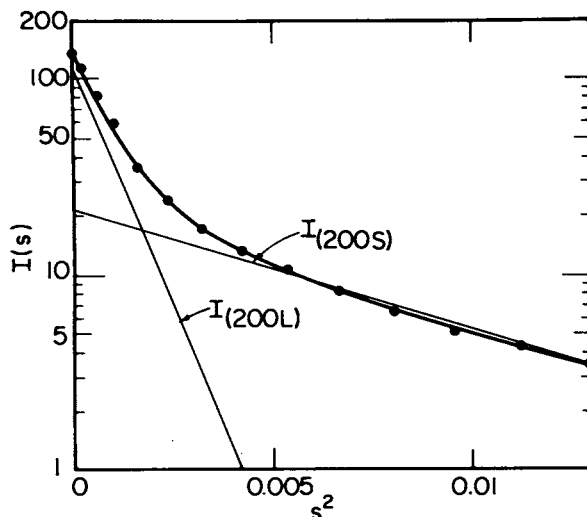


Fig. 4. Resolution of the (200) reflection profile into two Gaussian components by means of Guinier plot.

essentially disappeared, will the alkali begin to attack the larger crystallites during the slow phase of conversion, ultimately causing the disappearance of all cellulose I crystallites. The shift from the fast to the slow phase is reached at about the 65% conversion ratio,¹ i.e., the point where the small crystallites have been completely converted.

Because the average crystallite sizes determined by the procedures described in the previous paper are weight averages, and are thus influenced little by the relatively small amount of the smaller crystallites, the crystallite size of cellulose I appears to remain constant during the fast conversion phase. In the later, slow phase, the average size decreases quickly, indicating that crystallites of the larger size are being attacked by the alkali.¹

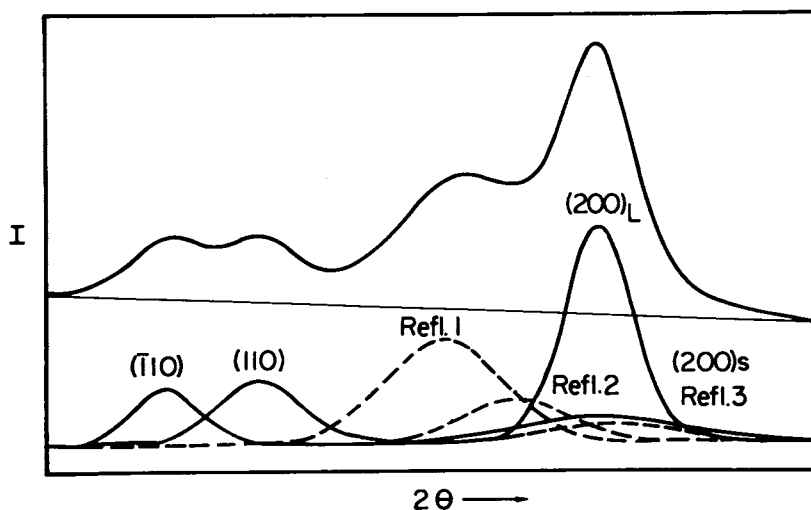


Fig. 5. Typical resolution of patterns of group A:—cellulose I reflections; (---) the Na-cellulose I reflections. (Also see caption of Fig. 1.)

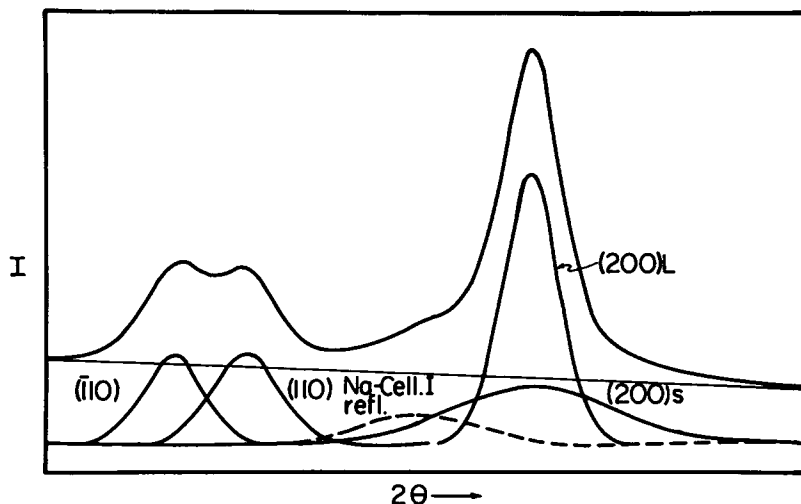


Fig. 6. Typical resolution of patterns of group B (also see captions of Figs. 1 and 5).

CONCLUSIONS

Previously, it had been proposed that mercerization of cellulose begins in the amorphous regions, at the interfaces between the crystallites.¹ This view is apparently correct, particularly in the light of the characteristics of the conversion during the first 20% (cf. Fig. 7). However, it also appears quite certain that very shortly after the onset of mercerization, the process continues by virtually destroying all of the small cellulose I crystallites. This part

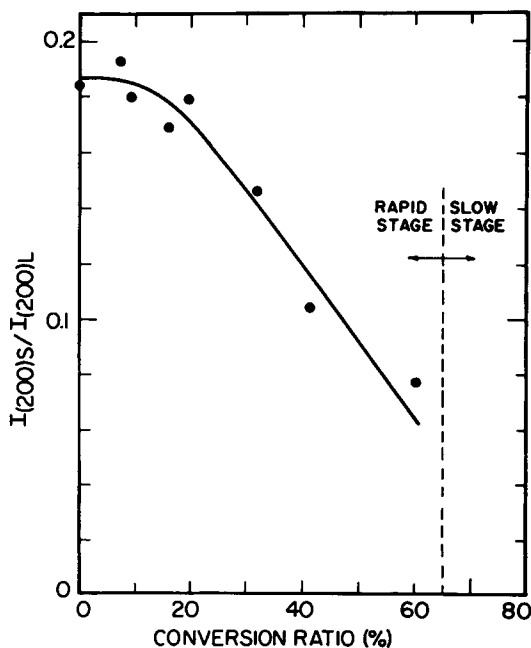


Fig. 7. The relationship between the intensity ratio $I_{(200)s}/I_{(200)L}$ and the conversion ratio.

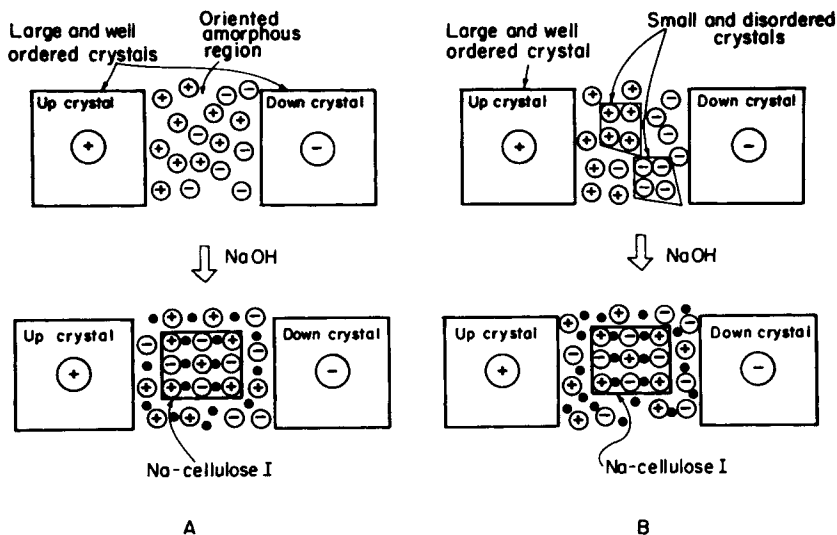


Fig. 8. A schematic representation of the probable mechanisms of conversion of cellulose I to Na-cellulose I, for (A) amorphous regions and (B) small crystallites.

of the process is relatively fast, occurring in about $1/7$ of the total conversion time.¹ This suggests that differences in the resistance to mercerization between the highly oriented amorphous regions and the small and disordered crystalline regions are small. Taken together, the nature of the solid-to-solid phase transformation, i.e., the conversion of a parallel-chain crystal structure to a (probably) antiparallel structure of Na-cellulose I is still the same. As was previously shown, the average crystallite diameter of Na-cellulose I reaches a value of ca. 35 \AA very early in the conversion process. This size can be very loosely interpreted as the average size of the amorphous regions in the fiber. (It should be noted that the average dimension of the small crystallites, 20 \AA , is considerably smaller than this value of 35 \AA .) These regions probably consist mostly of surface regions of the crystallites. Because the crystallite directions in the fiber are random along the fiber axis, approximately an equal number of "up" and "down" chains exists in these amorphous regions. The same is entirely true for the orientation of small (or any) crystallites. Therefore, the onset of mercerization in amorphous regions can draw on chains running in both directions—and continue on to small and disordered crystallites also running in both directions—thus forming an antiparallel Na-cellulose crystal structure with ease, as illustrated in Figure 8. For example, a rectangular amorphous area $35 \times 35 \text{ \AA}^2$ may contain from 30 to 40 cellulose chains, which is a sufficient number to begin forming a crystalline region.

These results indicate that the overall morphology of the ramie cellulose fiber may be subdivided into three regions—the highly oriented amorphous one, another consisting of small and disordered crystalline regions, and a third consisting of well-ordered crystalline regions. The differences between the former two regions are not distinct.

References

1. H. Nishimura and A. Sarko, *J. Appl. Polym. Sci.*, **33**, 855 (1986).
2. H. Nishimura, T. Okano, and I. Asano, *Jpn. Wood Research Soc.*, **28**, 659 (1982).
3. A. Sarko, FORTRAN computer program "LSQ", based on R. D. B. Fraser and E. Suzuki, *Anal. Chem.*, **38**, 1770 (1966).
4. C. Woodcock and A. Sarko, *Macromolecules*, **13**, 1183 (1980).
5. L. E. Alexander, *X-ray Diffraction Methods in Polymer Science*, Wiley, New York, 1969, p. 298.
6. R. B. Hanna and W. Cote, *Cytobiologie* **10**, 102 (1974).

Received July 2, 1986

Accepted July 9, 1986